LIMNOLOGY
AND
OCEANOGRAPHY

A consumer's guide to phytoplankton primary productivity models

Michael J. Behrenfeld and Paul G. Falkowski
Department of Applied Science, Oceanographic and Atmospheric Sciences Division, Brookhaven National Laboratory,
Upton, New York 11973-5000

Abstract

We describe a classification system for daily phytoplankton primary productivity models based on four implicit levels of mathematical integration. Depth-integrated productivity models have appeared in the literature on average once every 2 years over the past four decades. All of these models can be related to a single formulation equating depth-integrated primary production ($\Sigma\,PP$) to surface phytoplankton biomass (C_{surf}), a photoadaptive variable (P^b_{opt}), euphotic depth (Z_{eu}), an irradiance-dependent function (F), and daylength (DL). The primary difference between models is the description of F, yet we found that irradiance has a relatively minor effect on variability in $\Sigma\,PP$. We also found that only a small fraction of variability in $\Sigma\,PP$ can be attributed to vertical variability in phytoplankton biomass or variability in the light-limited slope for photosynthesis. Our results indicate that (1) differences between or within any model category have the potential to improve estimates of $\Sigma\,PP$ by $<10\%$, so long as equivalent parameterizations are used for C_{surf} and P^b_{opt}, and (2) differences in estimates of global annual primary production are due almost entirely to differences in input biomass fields and estimates of the photoadaptive variable, P^b_{opt}, not to fundamental differences between model constructs.

Models of daily phytoplankton carbon fixation are based on either idealized relationships between net photosynthesis and irradiance or measurements of net primary production. Net photosynthesis is estimated from the rate of O_2 evolution or ^{14}C uptake (Dring and Jewson 1982; Geider and Osborne 1992) measured during short (<2-h) incubations under a range of constant light intensities. The photosynthesis–irradiance relationships derived from these measurements can be used to estimate net primary production by calculating photosynthetic rates corresponding to changes in solar irradiance, integrating these photosynthetic rates over a photoperiod, and subtracting the daily respiratory costs associated with cell maintenance and growth. Alternatively, net primary production can be estimated directly from models based on measurements of ^{14}C uptake during 24-h incubations under variable solar irradiance.

By definition, net primary production is the amount of photosynthetically fixed carbon available to the first heterotrophic level and, as such, is the relevant metric for addressing environmental questions ranging from trophic energy transfer to the influence of biological processes on carbon

cycling (Lindeman 1942). Accordingly, many primary productivity models have been described. Unfortunately, the fundamental similarities and significant differences between models have been obscured by a tremendous diversity of variable names and parameterizations.

Here we examine relationships between productivity models and identify where improvements are most needed to enhance model performance. A coherent discussion of productivity models requires an organizational system for distinguishing between basic model categories, yet such a system does not exist. Thus, we begin our discussion by defining a classification scheme based on inherent levels of mathematical integration.

Categorization of productivity models

As a point of reference, we may consider the estimation of daily phytoplankton carbon fixation within the euphotic zone (Z_{eu} = penetration depth of 1% surface irradiance) per unit of ocean surface ($\Sigma\,PP$) as a common application for all primary productivity models. Extant models that can be used for such estimates range from simple relationships between surface chlorophyll concentration and $\Sigma\,PP$, to irradiance-dependent models of net photosynthesis integrated over time and based on fundamental photosynthetic parameters, such as functional absorption cross sections (σ_{PSII}) and electron turnover times (τ) for photosystem II. This wide spectrum of productivity models is often delineated into

Behrenfeld and Falkowski

I. Wavelength-resolved models (WRMs)

$$\Sigma PP = \int_{\lambda=400}^{700} \int_{t=\text{sunrise}}^{\text{sunset}} \int_{z=0}^{Z_{eu}} \Phi(\lambda, t, z) \times \text{PAR}(\lambda, t, z) \times a^*(\lambda, z)$$

$$\times \text{Chl}(z) \, d\lambda \, dt \, dz - R$$

II. Wavelength-integrated models (WIMs)

$$\Sigma PP = \int_{t=\text{sunrise}}^{\text{sunset}} \int_{z=0}^{Z_{eu}} \varphi(t, z) \times \text{PAR}(t, z) \times \text{Chl}(z) \, dt \, dz - R$$

II. Time-integrated models (TIMs)

$$\Sigma PP = \int_{z=0}^{Z_{eu}} P^b(z) \times \text{PAR}(z) \times DL \times \text{Chl}(z) \, dz$$

IV. Depth-integrated models (DIMs)

$$\Sigma PP = P^b_{opt} \times f[\text{PAR}(0)] \times DL \times \text{Chl} \times Z_{eu}$$

three categories: empirical, semianalytical, and analytical. However, the exact distinction between these categories is ambiguous because there are no truly analytical models based entirely on first principles (i.e. all extant models are dependent, at some level, upon empirical parameterizations).

We propose that a more rational categorization scheme can be devised based upon implicit levels of integration. The most fully expanded productivity models calculate net photosynthetic rates at discrete depths (z_i) within the illuminated region of a water body as a function of the wavelength-specific absorption of photosynthetically available radiation (PAR, 400–700 nm). These wavelength-resolved models (WRMs) convert absorbed radiation (i.e. photosynthetically utilizable radiation [PUR]; Morel 1978) into net photosynthesis using a suite of empirical quantum efficiency models based on photosynthesis–irradiance variables (e.g. P^b_{max}, α^b, β, E_k, ϕ_λ) (e.g. Sathyendranath and Platt 1989a; Sathyendranath et al. 1989; Morel 1991) or variables characterizing the photosystems (e.g. σ_{PSII}, τ) (Sakshaug et al. 1989; Dubinsky 1992). Daily water column primary production (Σ PP) is thus calculated by integrating photosynthetic rates over wavelength (λ), depth, and time (t) (Table 1):

$$\Sigma PP = \iiint f(\lambda_{\text{PUR}}, z_i, t) \, d\lambda \, dz \, dt. \tag{1}$$

The second model category results from removing the wavelength-dependence in Eq. 1, such that net photosynthesis is described as a function of PAR rather than PUR. These wavelength-integrated models (WIMs) calculate Σ PP by integrating PAR-dependent photosynthesis–irradiance functions over depth and time (Table 1):

$$\Sigma PP = \iint f(z_i, t) \, dz \, dt. \tag{2}$$

WIMs and WRMs are the only productivity models based on estimates of net photosynthesis (i.e. photosynthesis–irradiance measurements). Thus, only in WIMs and WRMs do the photosynthesis–irradiance variable names adhere to their accepted definitions: P^b_{max} is the chlorophyll-specific, light-saturated rate of photosynthesis as controlled by the cellular concentration and activity of enzymes involved in the dark reactions of carbon fixation, and α^b is the initial, light-limited slope for chlorophyll-specific carbon fixation and is related to the concentration of PSII reaction centers and σ_{PSII} (Falkowski 1992).

The third model category results from removing time-dependent resolution in solar irradiance. These time-integrated models (TIMs) retain vertical resolution but replace calculations of net photosynthesis with direct estimates of net primary production (Table 1):

$$\Sigma PP = \int f(z_i) \, dz. \tag{3}$$

Data used to parameterize TIMs come from measurements taken over extended periods (typically 6–24 h) under conditions of variable solar irradiance and thus have intrinsically integrated a range of photosynthetic rates into a single productivity value. Consequently, TIM variables are not equivalent to photosynthesis–irradiance variables. For example, the maximum primary production rate within a water column is not equivalent to the product of P^b_{max} and photoperiod. Rather, it reflects the optimum condition where the opposing effects of light limitation and photoinhibition are balanced to allow the maximum duration of photosynthesis at P^b_{max}.

Development of TIMs naturally followed the early observation that depth profiles of primary production typically exhibited predictable shapes similar to photosynthesis–irradiance functions (i.e. exhibiting regions of light saturation,

light limitation, and often photoinhibition) (Ryther 1956). Unfortunately, identical variable names were often adopted into TIMs along with the mathematical photosynthesis–irradiance formulations, despite the differences discussed above. These differences were notationally recognized as early as 1958 by Rodhe et al. and subsequently by Wright (1959), Vollenweider (1966, 1970), and Behrenfeld and Falkowski (1997), where maximum rates of daily photosynthesis within a water column were distinguished from P^b_{max} by replacing the subscript "max" with the subscript "opt" (*see* Vollenweider [1966, 1970] for discussions on the differences between TIM and photosynthesis–irradiance variables).

Depth-integrated models (DIMs) form the final category of daily productivity models and include all models lacking any explicit description of the vertically resolved components found in TIMs, WIMs, and WRMs. DIMs use vertically integrated functions to relate environmental variables measurable at the sea surface to $\Sigma\ PP$. The simplest DIMs calculate $\Sigma\ PP$ as a function of chlorophyll concentration alone (e.g. Smith and Baker 1978; Eppley et al. 1985) or the product of depth-integrated chlorophyll ($\Sigma\ C$) and daily integrated surface PAR (E_0) (e.g. Falkowski 1981; Platt 1986). More elaborate DIMs incorporate estimates of Z_{eu}, $\Sigma\ C$, and daylength, along with irradiance-dependent functions and photoadaptive parameters (e.g. Wright 1959; Platt and Sathyendranath 1993; Behrenfeld and Falkowski 1997) (Table 1).

In addition to the differences described above, WRMs and WIMs also differ from TIMs and DIMs in their requirement for explicitly correcting for autotrophic respiration. Integration of short-term photosynthesis–irradiance measurements over a photoperiod typically results in higher values for net primary production than observed from simultaneous 24-h ^{14}C uptake measurements. This discrepancy results from the calculated values not compensating for nocturnal respiratory losses of fixed carbon and because light respiration rates are increasingly underestimated during photosynthesis–irradiance measurements as incubation times decrease, due to a disequilibrium in the radiolabeling of cellular carbon pools. Consequently, parameterization of WRMs and WIMs using photosynthesis–irradiance data necessitates correction of $\Sigma\ PP$ estimates for autotrophic respiration (Table 1). In contrast, the multiple-hour ^{14}C uptake measurements used to parameterize TIMs and DIMs are presumed to intrinsically include autotrophic respiration (although this assumption is tenuous for incubations times $\ll 24$ h), and thus a correction for respiration is typically not included in $\Sigma\ PP$ estimates made with these models (Table 1).

The four model categories described above can be used to classify any daily productivity model. There is also a fifth model category, which we term annual production models (APMs). APMs relate annual average surface chlorophyll concentrations to annual primary production exported from the euphotic zone to depth (i.e. net annual community production) (Iverson and Esaias pers. comm.). APMs neglect changes in phytoplankton physiology on all space and time scales, as well as variability in surface irradiance and changes in phytoplankton biomass at subannual time scales. The following discussion and comparison of productivity models does not include APMs, but focuses on models of daily primary production, beginning with a description of the conceptual basis underlying DIMs.

Conceptual basis of depth-integrated models

A complete list of variables included in DIMs can be derived intuitively with only a fundamental understanding of phytoplankton photosynthesis. Explicitly, we would expect any model of water-column photosynthesis to require a measure of depth-integrated phytoplankton biomass, which, for practical purposes, can be estimated using the surface chlorophyll concentration (C_{surf}) scaled to the depth of the euphotic zone (Z_{eu}). We might also expect that an irradiance-dependent function [$f(E_0)$] and a photoadaptive yield term (e.g. P^b_{opt}) are required to convert the estimated biomass into a photosynthetic rate. Finally, we should include daylength (DL) as a variable, because DIMs are often parameterized and tested using observational data from multiple-hour incubations scaled to daily rates using daylength. Thus, the form of a complete DIM would be

$$\Sigma\ PP = C_{surf} \times Z_{eu} \times P^b_{opt} \times DL \times f(E_0). \qquad (4)$$

Although different parameterizations for each variable in Eq. 4 are found among the various published DIMs, the greatest source of diversity stems from differences in the description of $f(E_0)$. In the simplest case, $\Sigma\ PP$ is assumed to vary as a linear function of E_0 (e.g. Falkowski 1981), implying that either light saturation of photosynthesis does not occur or that variability in the light-saturated fraction of the euphotic zone does not significantly alter the average quantum yield of the water column. However, many DIMs recognize that the depth of light saturation varies as a function of E_0, and therefore include explicit parameterizations to account for this irradiance dependence. Talling (1957) presented an intuitive description of the relationship between E_0 and integral photosynthesis that was further developed by Vollenweider (1966, 1970) and is expanded upon here to derive the function $f(E_0)$.

Assuming no photoinhibition, the vertical profile of chlorophyll-normalized primary production (P_z^b) will exhibit a region of light saturation at the surface and a deeper region of light limitation. The P_z^b profile can be generalized to any water column by normalizing physical depths to optical depths (o.d. $= k_d \times z$, where k_d is the mean attenuation coefficient for PAR) (Fig. 1) and can be described using any one of the many photosynthesis–irradiance-type equations, such as (revised from Jassby and Platt 1976)

$$P_z^b = P^b_{opt} \times \tanh\ [E_z/E^*_k]. \qquad (5)$$

In Eq. 5, E_z is the average daily irradiance at depth z and E^*_k is the ratio of P^b_{opt} to the irradiance-dependent slope of the light-limited portion of the P_z^b profile and is used to delineate light-limitation from light saturation. The superscribed asterisk was added to E^*_k to distinguish it from the photosynthesis–irradiance variable, E_k ($=P^b_{max}/\alpha^b$), for the same reason that "opt" was added to distinguish P^b_{opt} from P^b_{max}.

Depth-integrated primary production ($\int_{z=0}^{\infty}\ P_z$) can be equated to the sum of areas for the two rectangles, A and B (Fig. 1), where A corresponds to the area of light saturation (as defined by E^*_k) and B to the area of light limitation. The horizontal dimension, ab, of both rectangles is equal to the product of $P^b_{opt} \times C_{surf} \times DL$. The vertical dimension, bc, is
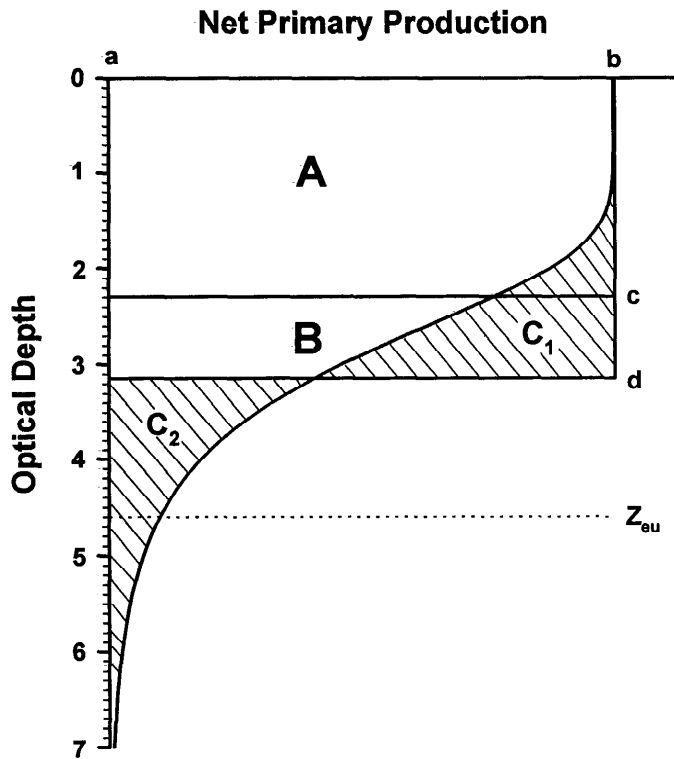
Net Primary Production

Fig. 1. Relationship between depth-integrated primary production ($\int_{z=0}^{\infty} P_z$) and rectangular equivalents. The curved line indicates the vertical profile of net primary production (P_z) calculated using Eq. 5 and plotted as a function of optical depth. $\int_{z=0}^{\infty} P_z$ is equal to the summed area of rectangles, A and B, which both have the horizontal dimension, $ab = P^b_{opt} \times DL \times C_{surf}$. The optical depth where subsurface irradiance is equal to E^*_k is indicated by c. The vertical dimension, bc, and thus the area of A, varies as a logarithmic function of surface irradiance (E_0), whereas the vertical dimension, cd, of B is approximately constant at $E_0 > E^*_k$. A value of $0.82/k_d$ for cd causes the shaded area, C_1, to equal the shaded area, C_2, when P_z is modeled using Eq. 5. Integration of P_z to the euphotic depth, Z_{eu}, (i.e. ΣPP) neglects production at optical depths >4.6 and thus causes cd to decrease with increasing E_0, although differences between ΣPP and $\int_{z=0}^{\infty} P_z$ are small.

the depth of light saturation and increases as a function of E_0 according to

$$\overline{bc} = \frac{\ln(E_0/E^*_k)}{k_d}. \tag{6}$$

In contrast, the vertical dimension, $\overline{cd}$, of rectangle B is essentially independent of E_0 for $E_0 > E^*_k$ and, when P_z^b is described by Eq. 5, $\overline{cd} \cong 0.82/k_d$. Combining terms for the two rectangles gives

$$\int_{z=0}^{\infty} P_z = \frac{P^b_{opt} \times C_{surf} \times DL}{k_d} \times [\ln(E_0/E^*_k) + 0.82]. \tag{7}$$

A slight error occurs when Eq. 7 is used to calculate ΣPP because truncating the P_z profile at the 1% light depth (i.e. Z_{eu}) causes cd to decrease linearly as E_0 increases. However, this error is only on the order of a few percentiles because the relative contribution of light-limited photosynthesis to Σ

PP decreases as E_0 increases. Thus, Eq. 7 can be converted into the form of Eq. 4 using the relationship $Z_{eu} = 4.6/k_d$:

$$\Sigma PP = C_{surf} \times Z_{eu} \times P^b_{opt} \times DL \times [0.22 \times \ln(E_0/E_k) + 0.18], \tag{8}$$

where $f(E_0)$ in Eq. 4 has been replaced by an explicit description of the E_0-dependent change in the light-saturated fraction of the euphotic zone.

Talling (1957) was the first to describe depth-integrated daily primary production using rectangular equivalents and derived, from planimetry, the equation

$$\int_{z=0}^{\infty} P_z = n \times P_m \times \frac{\ln(2)}{1.33 \times k_m} \times \left[\frac{\ln(E_0) - \ln(0.5 \times E^*_k)}{\ln(2)} \right], \tag{9}$$

where n is the concentration of phytoplankton (cells m^{-3}), P_m is the light-saturated photosynthetic rate per cell (mg O$_2$ cell^{-1} d^{-1}), and k_m is the attenuation coefficient for the deepest penetrating wavelength of PAR. The factor (1.33) is an empirical correction that roughly converts k_m to k_d. Rearranging terms and replacing n by C_{surf} and P_m by the product of P^b_{opt} [mg C (mg Chl)$^{-1}$ h^{-1}] and DL, Eq. 9 can be rewritten in the form of Eq. 7 as

$$\int_{z=0}^{\infty} P_z = \frac{P^b_{opt} \times C_{surf} \times DL}{k_d} \times [\ln(E_0/E^*_k) + 0.693]. \tag{10}$$

The lower value for $\overline{cd}$ in Eq. 10 (i.e. $0.693/k_d$), compared to Eq. 7, simply results from Talling's use of a photosynthesis–irradiance-type equation requiring a higher E_z for light saturation than does Eq. 5. Thus, the product $[C_{surf} \times P^b_{opt} \times DL \times k_d^{-1} \times \ln(E_z/E^*_k)]$ in Talling's model overestimates integral production above the depth of E^*_k more than in the model using Eq. 5 (i.e. rectangle A overestimates integral production from $z = 0$ to E^*_k more in Eq. 10 than in Eq. 7 simply due to differences in the photosynthesis–irradiance-type equation chosen to describe P_z^b), thereby requiring the lower value for cd in Eq. 10.

To facilitate model comparisons in the following sections, $f(E_0)$ can be expressed as the irradiance-dependent ratio between the mean photosynthetic rate within the euphotic zone and the maximum rate, P^b_{opt}. This ratio describes the loss in potential photosynthesis due to light limitation and is represented, for historical reasons (Wright 1959; Vollenweider 1966), by the variable F. We review the variety of published F functions in a latter section, but for now the meaning of F can be easily conceptualized from rectangular equivalents (Fig. 1) as:

$$F = \frac{\overline{bd}}{Z_{eu}}. \tag{11}$$

When $E_0 > E^*_k$ and photoinhibition is negligible, F increases according to $\ln(E_0/E^*_k)$ (Fig. 2), whereas the slope of F at lower irradiance is dependent upon the particular type of photosynthesis–irradiance equation used to describe P_z^b (see example above for Talling's equation). Eq. 8 can thus be rewritten:

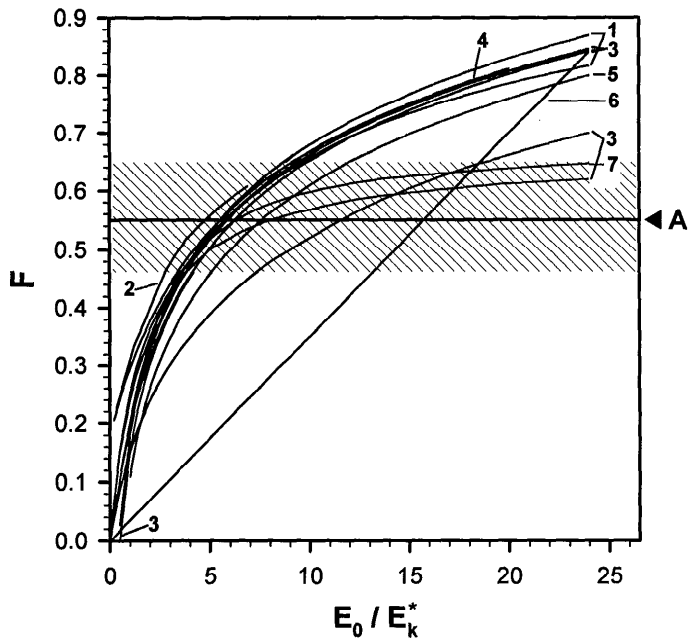$$\Sigma PP = C_{surf} \times Z_{eu} \times P^b_{opt} \times DL \times F, \tag{12}$$

Fig. 2. Summary of published estimates for the depth-integrated model (DIM) variable, F, expressed as a function of the ratio of surface irradiance (E_0) to the saturation irradiance (E_k^*). From rectangular equivalents (Fig. 1), F can be equated to the ratio of bd: Z_{eu}. Sources for each curve are (1) Eq. 8 integrated to 9 (top curve) and 4.6 optical depths (bottom curve), (2) Ryther and Yentsch's (1957) graphically represented variable, R, converted to F using the tabulated R values provided by Platt and Sathyendranath (1993: their table 2), (3) six models from Vollenweider (1966), (4) model of Platt and Sathyendranath (1993) converted to F by adding 0.82 and dividing by 4.6 optical depths, (5) Talling (1957), (6) linear irradiance dependence of ψ model (Falkowski 1981), and (7) Behrenfeld and Falkowski (1997). \\\\\ = range in observed F values reported by Rodhe et al. (1958), Wright (1959), Vollenweider (1966), and Rodhe (1966), with the median value of 0.55 indicated by horizontal solid line labeled A.

which we will refer to throughout the remainder of this article as the standard DIM equation.

Consolidating depth-integrated models

Diversity in approaches, inclusion of multiple levels of integration, and an inconsistency in the choice of variable names has made similarities between DIMs difficult to recognize. The purpose of this section is to illustrate the synonymy between DIMs by equating model variables and parameterizations to the standard DIM equation (Eq. 12), beginning with Talling (1957).

Talling (1957) derived a DIM from in situ vertical distributions of P_z and the photosynthesis–irradiance relationship originally presented by Smith (1936). Oxygen evolution data used by Talling were from incubations sufficiently short to require correction for respiration when extrapolated to estimates of Σ PP (*see* Talling's eq. 2), but the measurements were made under variable irradiance so that the standard interpretation of DIM variables holds (*see above*) despite Talling's use of photosynthesis–irradiance variable names

(e.g. $P_m \equiv P^b_{opt}$). We already described the synonymy between Talling's DIM (Eq. 9) and Eq. 12, but failed to recognize several of Talling's additional significant conclusions. For example, he suggested that variability in the slope of the light-limited portion of the water column had only a minor effect on Σ PP. In addition, an efficiency factor (f) was defined for the water column describing the loss of potentially usable PAR due to light saturation (although Talling's f differs from the F function in Eq. 12 that describes the loss of potential production due to light-limitation).

A second DIM was published in 1957 by Ryther and Yentsch, which expanded upon the earlier model of Ryther (1956) by expressing Σ PP (g C m^{-3} d^{-1}) as a function of chlorophyll:

$$P = R/k \times C \times p(\text{sat}),\qquad(13)$$

where $P \equiv \Sigma$ PP, $k \equiv k_d$, C is the chlorophyll concentration when biomass is distributed evenly through the water column $\equiv C_{surf}$, $p(\text{sat})$ is the light-saturated rate of photosynthesis assuming no photoinhibition (g C m^{-3} h^{-1}) $\equiv P^b_{opt}$, and R is the change in integral photosynthesis as a function of E_0 (which was presented graphically). Although it was not noted in the original report, R has units of hours per day (i.e. R incorporates DL). Thus, by converting k into Z_{eu}, dividing R by the optical depth of the euphotic zone (i.e. 4.6), and extracting DL from R, Eq. 13 becomes synonymous with Eq. 12.

In 1959, Wright reported an equation for Σ PP that has remained relatively unrecognized but is nearly identical to Eq. 12. Wright used oxygen evolution data collected in Canyon Ferry Reservoir (Montana) to derive the DIM (his eq. 4):

$$\Sigma P = \frac{4.6}{k} \times F \times T \times C \times R_{opt},\qquad(14)$$

where Σ $P \equiv \Sigma$ PP, $C \cong C_{surf}$, $R_{opt} \equiv P^b_{opt}$, and T is the number of hours of daily photosynthesis $\cong DL$ (although Wright cautioned against substituting DL for T due to changes in photosynthetic rates over the day). Eq. 14 is the first appearance of the factor, F, which he described as the "ratio of euphotic zone to optimal photosynthesis." Surprisingly, Wright stated that no relationship could be observed between F and E_0 and suggested that a better correlation existed between F and surface temperature. However, he used monthly average values for F and E_0 in this comparison, which may have partially masked E_0 dependence. More importantly, Wright found that the average value of F was ~0.54, with a range of 0.35–0.63 (we note that F values given in Wright's table 8 are slightly erroneous based on values of Σ PP, P^b_{opt}, and k_d in the same table). As will be seen below, similar estimates for the mean value of F are recurrent in DIM parameterizations.

Wright's use of the variable R_{opt}, as a distinction from the photosynthesis–irradiance variable P^b_{max}, was preceded by that of Rodhe et al. (1958) in their equation, which was parameterized using ^{14}C measurements from Lake Erken, Sweden:

$$\Sigma a = (2.4\text{–}2.7) \times \frac{a_{opt}}{\epsilon},\qquad(15)$$

where Σ $a \equiv \Sigma$ PP, $\epsilon \equiv k_d$, and $a_{opt} \equiv P^b_{opt} \times C_{surf} \times DL$.

The range 2.4–2.7 is an estimate of the product $4.6 \times F$, which gives a range for F of 0.52–0.58. Thus, Eq. 15 is equivalent to Eq. 12. Rodhe et al. concluded that potential variability in $\Sigma \; PP$ was greatly restricted by physiological acclimations and that $\Sigma \; PP$ was largely independent of day-to-day variability in surface light intensities.

Rodhe et al.'s distinction between P^b_{opt} and P^b_{max} was abandoned in a subsequent report by Rodhe (1966), where a_{opt} was replaced by the variable a_{max}. In this often-cited publication, Rodhe adopted Talling's conceptual model for $\Sigma \; PP$ and focused primarily on parameterizing the function F by using carbon assimilation measurements from 12 European lakes with a wide range of optical properties. Rodhe's equation for integral production was

$$\Sigma \; a = z_{0.5 \; Ik} \times a_{max}, \tag{16}$$

where $\Sigma \; a \equiv \Sigma \; PP$, $a_{max} \equiv P^b_{opt} \times C_{surf} \times DL$, and $z_{0.5 \; Ik}$ is the depth corresponding to an average light intensity of $0.5 \times E^*_k \equiv F \times 1/k_d$. Thus, Eq. 16 can be equated to Eq. 12 when $1/k_d$ is converted into Z_{eu}.

By using data from 9 of the 12 study lakes, Rodhe (1966) calculated an average $z_{0.5 \; Ik}$ of 2.3 o.d., with a range of 2.1–3.0 o.d. (*see* Rodhe's table 1, but note that o.d. was not expressed in the current standard format $[-k^*_a z]$ and attenuation coefficients were for the deepest penetrating wavelength, not k_d). These $z_{0.5 \; Ik}$ values correspond to an average F of 0.5 and range of 0.46–0.65, which is similar to the results of Rodhe et al. (1958), Wright (1959), and Vollenweider (1966: range, 0.54–0.65). Rodhe (1966) concluded that using a mean $z_{0.5 \; Ik}$ equivalent to an F value of 0.5 would not introduce significant errors in estimates of $\Sigma \; PP$ (however, we note that all productivity profiles used in this computation exhibited light saturation to ~ 1.4 standard o.d., indicating a lack of data from low light conditions; *see* Rodhe's Fig. 4). Rodhe also calculated that productivity at depths $> Z_{eu}$ contributed negligibly to $\Sigma \; PP$ and nicely illustrated the minimal variability exhibited in the light-limited slope of P_z (*see* Rodhe's fig. 8).

In the same year, Vollenweider (1966) published the standard DIM equation from expressions for the depth-dependent changes in net photosynthesis. His basic formulation for $\Sigma \; PP$ was

$$\sum P = F(i) \times \frac{P_{opt}}{\epsilon}, \tag{17}$$

where $\Sigma \; P \equiv \Sigma \; PP$, $P_{opt} \equiv P^b_{opt} \times C_{surf} \times DL$, $\epsilon \equiv k_d$, and $F(i) \equiv 4.6 \times F$ from Eq. 12. Vollenweider concluded that variations in the vertical distribution of P_z had little impact on variability in $\Sigma \; PP$, such that changes in P_{opt} were of much greater importance than photoinhibition or the degree of acclimation to low light.

In the early 1970s, modeling efforts began to focus on the expansion of standard DIM variables in an attempt to improve model performance. For example, Vollenweider (1970) separated the compound variable, k_d, into attenuation due to phytoplankton chlorophyll (η_π) and that due to water, dissolved organics, and detritus (ϵ). The resultant DIM was

$$\sum A = \frac{\pi_{opt} \times b}{\epsilon + \eta_\pi \times b} \times F(I_0/I_k), \tag{18}$$

where $\Sigma \; A \equiv \Sigma \; PP$, $\pi_{opt} \equiv P^b_{opt} \times DL$, $b \equiv C_{surf}$, and $F(I_0/I_k) \equiv 4.6 \times F$. The variable η_π has units of $m^2 \; (mg \; Chl)^{-1}$ and has subsequently been given a variety of names, such as k_n, k_c, a^*, and c_{ph}. Eq. 18 was the first of a long line of productivity models attempting to improve $\Sigma \; PP$ estimates by partitioning subsurface light attenuation to account for chlorophyll-dependent variability in the relative fraction of incident PAR absorbed by phytoplankton.

Megard (1972) combined Eq. 10 and 18 into the abbreviated DIM:

$$\Sigma \; P = a \times \exp(-k_n n) \times p_{max}, \tag{19}$$

where $\Sigma \; P \equiv \Sigma \; PP$, $a \equiv 4.6 \times F \times \epsilon^{-1}$, $k_n n \equiv \eta_\pi \times b$, $p_{max} \equiv P^b_{opt} \times C_{surf} \times DL$, and ϵ, η_π, and b are as defined above. Megard calculated an average k_n value of 0.013 (based on ^{14}C measurements from Lake Minnetonka, Minnesota), which is similar to later estimates by Talling (1970), M. Lorenzen (1972), C. J. Lorenzen (1972), and Smith and Baker (1978).

Bannister (1974) equated $\Sigma \; PP$ to the realized fraction of light absorbed by phytoplankton and a maximum obtainable limit to daily production when all available radiation is absorbed by phytoplankton:

$$\Pi = \Psi \times \frac{k_c C}{k_c C + k_w}, \tag{20}$$

where $\Pi \equiv \Sigma \; PP$, k_c and $k_w \equiv \eta_\pi$ and ϵ in Eq. 18, respectively, and C is the chlorophyll concentration. Based on Rodhe's (1966) average $z_{0.5 \; Ik}$ of 2.3, the upper limit to production (Ψ) was estimated as

$$\Psi = 2.3 \times P_{max} \times k_c^{-1}, \tag{21}$$

where $P_{max} \equiv P^b_{op.} \times DL$. Similarity between Eq. 21 and the relationship

$$\Sigma \; PP = 2.3 \times P_{max} \times k_d^{-1}, \tag{22}$$

where $P_{max} \equiv P^b_{opt} \times C_{surf} \times DL$, has subsequently resulted in Eq. 22 being erroneously credited to Bannister (e.g. Banse and Yong 1990; Balch et al. 1992) rather than to Rodhe (1966).

Productivity modeling efforts bifurcated during the later half of the 1970s. In one direction, physical principles of spectral light attenuation were applied to $\Sigma \; PP$ models to improve the characterization of subsurface irradiance over that achieved by Eq. 18–20. These efforts reflected the coincident improvements being made in the measurement and modeling of marine optics and culminated into the so-called bio-optical models (i.e. WRMs) discussed by Morel (1991) and reviewed by Bidigare et al. (1992). The other direction of model development was motivated by the availability of satellite ocean color data and resulted in simplified DIMs relating $\Sigma \; PP$ to satellite-derived sea-surface chlorophyll concentrations.

In 1978, Smith and Baker published a model for $\Sigma \; PP$ (their variable, P_z) based entirely on the average chlorophyll concentration within the upper attenuation length (C_k):

$$P_T = 1.254 + 0.728 \times \log(C_k). \tag{23}$$

A similar model was later published by Eppley et al. (1985):

$$\log (\Pi) = 3 + 0.5 \times \log(C_k), \tag{24}$$

where $\Pi \equiv \Sigma \; PP$. Eq. 23 and 24 are the simplest form of

DIMs and neglect all variability in $\Sigma\,PP$ due to irradiance, daylength, and the photoadaptive state of phytoplankton. In certain cases, chlorophyll-based models provide reasonable estimates of $\Sigma\,PP$ (e.g. Smith and Baker 1978; Eppley et al. 1985), but in other cases they account for $<50\%$ of the variability in $\Sigma\,PP$ (e.g. Banse and Yong 1990; Balch et al. 1992; Behrenfeld and Falkowski 1997). Smith and Baker (1978) recognized the deficiencies of Eq. 23 and suggested improvements focusing on the fractional absorption of available light by phytoplankton (as in Eq. 18–20). Eppley et al. (1985) also expanded their model (Eq. 24) to include parameterizations for sea-surface temperature anomalies and daylength (their eq. 1 in table 4).

Another simplified form of the standard DIM is the ψ model described by Falkowski (1981):

$$P = \psi \times B \times E_0, \tag{25}$$

where $P \equiv \Sigma\,PP$ and B = chlorophyll concentration integrated from $z = 0$ to Z_{eu} (i.e. $\Sigma\,C$). The ψ model implicitly assumes a constant photoadaptive state for the water column and a linear dependence of $\Sigma\,PP$ on E_0. Recognizing that $\Sigma\,C \cong C_{surf} \times Z_{eu}$, Eq. 25 can be restated as

$$\Sigma\,PP = \psi \times E_0 \times C_{surf} \times Z_{eu} \tag{26}$$

and, from Eq. 12 and 26,

$$\psi \times E_0 = P^b_{opt} \times DL \times F. \tag{27}$$

Falkowski (1981) reported a value of $\psi = 0.43$ g C (g Chl)$^{-1}$ (mol quanta)$^{-1}$ m^{-2} for a range in E_0 from <10 to >70 mol quanta m^{-2} d^{-1}. Taking, then, a central value of $E_0 = 35$ mol quanta m^{-2} d^{-1} and assuming an average value for F of 0.5 (Rodhe 1966), the irradiance-dependent slope included within the variable ψ is $0.5/35 = 0.014$ (Fig. 2). For an average daylength of 12 h, Falkowski's ψ model assumes a constant P^b_{opt} value of roughly $\psi/(0.014 \times 12) = 2.5$ g C (g Chl)$^{-1}$ h^{-1}. This P^b_{opt} value is at the lower end of the range observed by Behrenfeld and Falkowski (1997) for their dataset of $\sim1,700$ productivity profiles. For comparison, the ψ range of 0.31–0.66 reported by Platt (1986) corresponds to a P^b_{opt} range of 1.8–3.8 g C (g Chl)$^{-1}$ h^{-1} when calculated using the E_0, DL, and F values above. Morel (1991) further investigated variability in ψ using a WRM and found that ψ was not a linear function of irradiance, but increased strongly as irradiance decreased (note that Morel's ψ^* is identical to ψ in Eq. 25 except that photosynthetically fixed carbon is converted to energetic equivalents following Platt and Irwin [1973]).

In 1990, Banse and Yong applied the DIM of Rodhe (1966) to describe variability in $\Sigma\,PP$ observed in the eastern tropical Pacific ocean as

$$P_t = 2.3 \times (P/Chl)_{opt} \times Pig_{sat} \times k^{-1}, \tag{28}$$

where $P_t \equiv \Sigma\,PP$, $Pig_{sat} \equiv C_{surf}$ and $k \equiv k_d$. They used the variable $(P/Chl)_{max}$ as a correlate for P^b_{opt}, whereas $(P/Chl)_{opt}$ in Eq. 28 signifies the maximum value of P_z between 0.69 and 1.3 o.d. The distinction between $(P/Chl)_{max}$ and $(P/Chl)_{opt}$ was made because Banse and Yong believed that the occurrence of $(P/Chl)_{max}$ at >1.3 o.d. reflected experimental artifacts resulting from incubations at sea-surface temperatures of samples collected from the thermocline.

The principal conclusion of Banse and Yong (1990) was that variability in $\Sigma\,PP$ resulted almost entirely from variability in P^b_{opt} and was independent of $\Sigma\,C$, E_0, and DL. However, this counterintuitive conclusion is not as surprising as it might first appear because, for their dataset, DL was essentially constant, E_0 showed only minor fluctuations, and $\Sigma\,C$ only varied from ~10 to 20 mg Chl m^{-2} (compared to the global range in $\Sigma\,C$ of >2.5 orders of magnitude).

Platt and Sathyendranath (1993) used dimensional analysis to derive the relationship:

$$P_{z,t} \sim \frac{B \times P^b_m \times D}{K} \times f(I_*^m), \tag{29}$$

where $P_{z,t} \equiv \Sigma\,PP$, $B \equiv C_{surf}$ for a uniformly distributed biomass, $D \equiv DL$, $K \equiv k_d$, $P^b_m \equiv P^b_{max}$, and I_*^m = the ratio of modeled clear sky irradiance at local noon to E_k. Differences between P^b_{max} and P^b_{opt} were assumed to be captured by the function $f(I_*^m)$. Tabulated values for $f(I_*^m)$ were shown to be nearly identical to the converted F functions of Talling (1957) and Rodhe (1966). Thus, Eq. 29 can be related to the standard DIM by changing $1/k_d$ into Z_{eu}, replacing P^b_{max} with P^b_{opt}, and converting $f(I_*^m)$ into F using Eq. 5 to describe the irradiance dependence of P_z (Fig. 2). An important contribution of Platt and Sathyendranath (1993) was the evaluation of variability in E_k and I_*^m using data from $\sim1,000$ photosynthesis–irradiance measurements conducted on natural phytoplankton assemblages. They found that I_*^m only ranged from 3.2 to 15 when E_k values were averaged over the upper 40 m of the water column. Recognizing that I_*^m is proportional E_0/E_k^*, these results indicate that variability in E_0/E_k^* is far more constrained than E_k^* alone.

Behrenfeld and Falkowski (1997) empirically derived a TIM describing observed vertical variability in P_z. However, comparison of model performance using structured and uniform chlorophyll profiles indicated that including biomass profiles did not significantly improve estimates of $\Sigma\,PP$. Therefore, they reduced their TIM to the DIM:

$$\Sigma\,PP = C_{surf} \times Z_{eu} \times P^b_{opt} \times DL \times \left[\frac{0.66125 \times E_0}{E_0 + 4.1}\right], \tag{30}$$

where the E_0-dependent term in brackets is an estimate of F. We calculated an average value for F of 0.55 for the database of Behrenfeld and Falkowski.

To summarize this section, all published DIMs can be transformed into a single standard model (Eq. 12). Recognizing synonymy between DIMs requires the identification of equivalent variable names (Table 2) and an association between empirical constants and DIM variables. Mathematical derivations based on photosynthesis–irradiance relationships typically result in fully expressed DIMs, whereas observationally based models commonly substitute DIM variables with constants. In most cases, DIMs differ primarily in the estimation of the photoadaptive parameter, P^b_{opt}, and description of the irradiance-dependent function F.

The F function

Light intensity affects $\Sigma\,PP$ in two ways: it influences the photoadaptive state of phytoplankton and it controls the rel-

Table 2. Consolidation of depth-integrated model (DIM) variables by equating published variable names with those used in the standard DIM (Eq. 12).

Variable	Definition	Units
Standard DIM variables		
$\Sigma\,PP$	Daily carbon fixation integrated from the surface to Z_{eu}	mg C m^{-2} d^{-1}
C_{surf}	Chlorophyll concentration measured at the depth nearest the surface or as derived by satellite	mg Chl m^{-3}
Z_{eu}	Physical depth receiving 1% of surface irradiance. Equivalent to 4.6 divided by the mean attenuation coefficient for PAR (i.e. k_d).	m
P^b_{opt}	Maximum chlorophyll-specific carbon fixation rate observed within a water column measured under conditions of variable irradiance during incubations typically spanning several hours. P^b_{opt} differs from the photosynthesis–irradiance variable, P^b_{max}, which is measured during short incubations (≤ 2 h) under constant irradiance. P^b_{max} reflects the light-saturated rate of carbon fixation as physiologically controlled by the capacity of the photosynthetic dark reactions.	mg C (mg Chl)$^{-1}$ h^{-1}
DL	Daylength or photoperiod	h
F	Relative fraction of potential photosynthesis lost within the euphotic zone due to light limitation. To first order, F = average production of the water column divided by P^b_{opt}.	Unitless
E^*_k	Light intensity corresponding to the intersection between the light-limited slope of carbon fixation observed within a water column and P^b_{opt}.	mol photons m^{-2} d^{-1}

Description	Variable	Source	Units	Approx. std. equivalents
Synonymous DIM variables				
Biomass	n	Talling 1957	cells m^{-3}	C_{surf}*
		Megard 1972	mg Chl m^{-3}	C_{surf}
	C	Ryther and Yentsch 1957	g Chl m^{-3}	C_{surf}
		Wright 1959		
		Bannister 1974		
	C_k	Smith and Baker 1978	mg Chl m^{-3}	C_{surf}
		Eppley et al. 1985		
	B	Vollenweider 1970	mg Chl m^{-3}	C_{surf}
		Platt and Sathyendranath 1993		
		Falkowski 1981	g Chl m^{-2}	$C_{surf} \times Z_{eu}$
	Pig_{sat}	Banse and Yong 1990	mg Chl m^{-3}	C_{surf}
Photoadaptive variable	P_m	Talling 1957	mg O$_2$ cell^{-1} d^{-1}	$P^b_{opt} \times DL$†
	$p(sat)$	Ryther and Yentsch 1957	g C (g Chl)$^{-1}$ h^{-1}	P^b_{opt}
	a_{opt}	Rodhe et al. 1958	g C m^{-3} d^{-1}	$P^b_{opt} \times DL \times C_{surf}$
	R^b_{opt}	Wright 1959	μmol O$_2$ (μg Chl)$^{-1}$ h^{-1}	P^b_{opt}
	a_{max}	Rodhe 1966	mg C m^{-3} d^{-1}	$P^b_{opt} \times DL \times C_{surf}$
	π_{opt}	Vollenweider 1970	mg C (mg Chl)$^{-1}$ d^{-1}	$P^b_{opt} \times DL$
	P_{max}	Megard 1972	g C (g Chl)$^{-1}$ d^{-1}	$P^b_{opt} \times DL$
		Bannister 1974	mg C m^{-3} d^{-1}	$P^b_{opt} \times DL$
	p_{max}	Megard 1972	mg C m^{-3} d^{-1}	$P^b_{opt} \times DL \times C_{surf}$
		Bannister 1974	mg C m^{-3} d^{-1}	(NSEq)‡§
	p_{opt}	Bannister 1974	mg C m^{-3} d^{-1}	(NSEq)#
	Ψ	Falkowski 1981	g C (g Chl)$^{-1}$ mol quanta^{-1} d^{-1}	$(P^b_{opt} \times DL \times F)/E_0$
	$(P/Chl)_{max}$	Banse and Yong 1990	mg C (mg Chl)$^{-1}$ d^{-1}	$P^b_{opt} \times DL$
	$(P/Chl)_{max}$	Banse and Yong 1990	mg C (mg Chl)$^{-1}$ d^{-1}	(NSEq)¶
	P^b_m	Platt and Sathyendranath 1993	mg C (mg Chl)$^{-1}$ d^{-1}	(NSEq)§
Mean PAR attenuation coefficient	$k_m \times 1.33$	Talling 1957	m^{-1}	$Z_{eu} = 4.6/(1.33 \times k_m)$
	K_T	Smith and Baker 1978	m^{-1}	$Z_{eu} = 4.6/K_T$
	ϵ	Rodhe et al. 1958	m^{-1}	$Z_{eu} = 4.6/\epsilon$
	k	Ryther and Yentsch 1957	m^{-1}	$Z_{eu} = 4.6/k$
		Wright 1959		
		Banse and Yong 1990		
		Platt and Sathyendranath 1993		
	$k_n n + k_w$	Vollenweider 1970	m^{-1}	$Z_{eu} = 4.6/(k_n n + k_w)$
		Megard 1972		
	$k_c C + k_w$	Bannister 1974	m^{-1}	$Z_{eu} = 4.6/(k_c C + k_w)$
Average spectral extinction	η_π	Vollenweider 1970	m^2 (mg Chl)$^{-1}$	(NSEq)**
Coefficient for chlorophyll	k_n	Megard 1972	m^2 (mg Chl)$^{-1}$	(NSEq)
	k_c	Bannister 1974	m^2 (mg Chl)$^{-1}$	(NSEq)

Table 2. Continued.

Description	Variable	Source	Units	Approx. std. equivalents
Irradiance-dependent function	R	Ryther and Yentsch 1957	h d^{-1}	$4.6 \times F \times DL$
	$F(i)$	Vollenweider 1970	Unitless	$4.6 \times F$
Hours of daily photosynthesis	T	Wright 1959	h d^{-1}	DL
	D	Platt and Sathyendranath 1993	h d^{-1}	DL
Depth-integrated production	$\int_z \int P \, dz \, dt$	Talling 1957	mg O$_2$ m^{-2} d^{-1}	Σ PP††
	Σa	Rodhe et al. 1958 Rodhe 1966	mg C m^{-2} d^{-1}	Σ PP
	ΣA	Vollenweider 1970	(Not specific)	Σ PP
	Σp	Wright 1959	mmol O$_2$ m^{-2} d^{-1}	Σ PP
		Megard 1972 Vollenweider 1966	g C m^{-2} d^{-1}	Σ PP
	Π	Bannister 1974	g C m^{-2} d^{-1}	Σ PP
		Eppley et al. 1985	mg C m^{-2} d^{-1}	
	P_T	Smith and Baker 1978 Banse and Yong 1990	mg C m^{-2} d^{-1}	Σ PP
	P	Ryther 1956 Ryther and Yentsch 1957 Falkowski 1981	g C m^{-2} d^{-1}	Σ PP
	$P_{Z,T}$	Platt and Sathyendranath 1993	mg C m^{-2} d^{-1}	Σ PP††

* Biomass variables are assigned standard equivalent variables assuming a uniform biomass profile.

† Standard equivalent only approximate due to differences between O$_2$ evolution and carbon fixation.

‡ NSEq = no standard DIM equivalent.

§ Synonymous variable name equivalent to the photosynthesis–irradiance variable, P^b_{max} (*see* Categorization of productivity models).

\# Synonymous variable name equivalent to the maximum photosynthetic rate when photoinhibition is significant.

¶ Synonymous variable name equivalent to the maximum daily primary production observed between 0.69 and 1.3 optical depths.

** Average spectral extinction coefficients for chlorophyll are used in conjunction with chlorophyll concentration and the extinction coefficient for water to derive Z_{eu} and the fraction of light absorbed by phytoplankton.

†† Depth integration of daily primary production extended to infinity, rather than Z_{eu}, as in Eq. 7.

ative depth of light-saturation. In DIMs, the F function attempts to account for the latter phenomenon. Differences in F functions are due to variations in the photosynthesis–irradiance-type equation used to describe P_z or assumptions regarding the importance of an irradiance-dependent term in modeling Σ PP. Let us now compare different F functions and assess their implications on Σ PP estimates.

Assuming no photoinhibition, we showed that F is solely a function of $\ln(E_0/E_k^*)$ when E_0 exceeds E_k^* (Eq. 7). Accordingly, the same curvature above E_k^* is exhibited in the F functions described by Talling (1957), Vollenweider (1966), and the converted function of Platt and Sathyendranath (1993) (Fig. 2). Minor discrepancies in the magnitude of these F functions and their curvature at low E_0 result from differences in the presumed kinetics of photosynthesis under subsaturating light. Including photoinhibition, as in the F functions derived by Ryther and Yentsch (1957), Vollenweider (1966), and Behrenfeld and Falkowski (1997), results in a more gradual rate of increase in F as E_0 increases above E_k^*, thereby reducing the irradiance dependence of Σ PP (Fig. 2). In contrast to these explicit functions, Rodhe et al. (1958), Wright (1959), and Rodhe (1966) assigned average values or ranges to F that, when combined, yield a median of 0.55 and a typical range of 0.46–0.65 (Fig. 2).

By using the dataset compiled by Behrenfeld and Falkowski (1997) and Eq. 12, we investigated whether differences between the F functions illustrated in Fig. 2 significantly affect model estimates of Σ PP. To restrict this analysis to differences in F functions alone, all calculations were based on measured values of C_{surf}, Z_{eu}, P^b_{opt}, and E_0,

and compared to measured Σ PP with and without photoinhibition. Similar to Platt and Sathyendranath (1993), Behrenfeld and Falkowski (1997) found a linear relationship between E_0 and E_k^*:

$$E_k^* = 0.046 \times E_0 + 0.68, \qquad (31)$$

which was, therefore, applied to each F function. Results from this comparison indicated equivalent correlation coefficients between modeled and measured Σ PP ($r^2 = 0.86$) for all F functions except the linear function implicated by the ψ model (Eq. 25), which reduced model performance by 14% (i.e. $r^2 = 0.72$). In contrast, model performance was reduced by only 3% (i.e. $r^2 = 0.83$) when Σ PP was estimated using a constant value of $F = 0.55$. We therefore conclude that (1) For most practical purposes, changes in surface PAR have a relatively minor effect on variability in Σ PP. Thus, we can expect that increasing the time, depth, or wavelength resolution in model descriptions of PAR will not significantly improve estimates of Σ PP, unless the increased resolution directly improves the characterization of the photoadaptive variables E_k^* or P^b_{opt}. (2) Reported differences in DIM performance (e.g. Balch et al. 1992) do not result from fundamental differences in model structure, but rather reflect differences in the parameterization of the photoadaptive variables.

Vertically resolved productivity models

Vertically resolved productivity models (i.e. TIMs, WIMs, WRMs) attempt to improve estimates of Σ PP by accounting for depth-dependent changes in phytoplankton biomass (C_z)

and physiological adjustments to subsurface irradiance [$f(E_z)$]. As DIMs can account for ~85% of the observed variability in $\Sigma\ PP$ (*see above*), the maximum unexplained variance that can be attributed to variability in C_z and $f(E_z)$ combined is only ~15%.

DIMs implicitly assume a vertically homogeneous distribution of biomass, which has long been recognized as an oversimplification. Numerous C_z models have thus been developed, such as the C_{sat}-based Gaussian distributions described by Platt and Sathyendranath (1988) and Morel and Berthon (1989). Sensitivity analyses by Platt et al. (1991) and Antoine et al. (1996) indicated that model estimates of $\Sigma\ PP$ differed by <20% for calculations based on structured C_z profiles compared to vertically homogeneous distributions. The largest discrepancies occurred when modeled chlorophyll maxima were near the surface, yet sufficiently deep to prevent detection by satellites (Platt and Sathyendranath 1988). Differences in $\Sigma\ PP$ estimates were smaller for the more common situation of chlorophyll maxima near the base of the euphotic zone. These effects of vertical variability in C_z on P_z are of relatively minor importance to total variability observed in $\Sigma\ PP$. We found that, of the ~15% variance in $\Sigma\ PP$ unexplained by the standard DIM (Eq. 12), ~4% could be accounted for by replacing uniform C_z profiles with measured C_z values in the vertically resolved model of Behrenfeld and Falkowski (1997), even when large coastal components of the dataset were removed for the comparison.

Combining the variance explained by Eq. 12 (~85%) and that attributable to C_z (~5%) leaves an unexplained variance in $\Sigma\ PP$ of ~10%, a fraction of which can be attributed to spatial (i.e. horizontal) variability in E_k^* not accounted for by Eq. 31 and vertical variability in E_k^* resulting from depth-dependent photoadaptive changes within the phytoplankton community in response to light limitation. Of these, characterization of $f(E_z)$ in vertically resolved models can improve estimates of $\Sigma\ PP$ over those of DIMs only as a result of improved descriptions of the light-limited slope of P_z, because improved descriptions of spatial variability in E_k^* can be effectively incorporated into DIMs (e.g. Eq. 31).

The relative importance of variability in E_k^* can be constrained by calculating $\Sigma\ PP$ for two P_z profiles modeled with vertically uniform light-limited slopes differing by a factor of six (i.e. the maximum range expected in situ) and having identical values for P^b_{opt} (Fig. 3). By using the TIM of Behrenfeld and Falkowski (1997) and assuming a homogeneous C_z distribution, $\Sigma\ PP$ for the two profiles differs by a factor of ~1.5–3 for E_0 ranging from 65 to 5 mol quanta m^{-2}, respectively. These differences in $\Sigma\ PP$ represent the maximum variability attributable to photoadaptive responses to light-limitation when C_z is uniform. In the same manner, P_z can be calculated for a water column with a vertical gradient in the light-limited slope, increasing by a factor of 6 from the surface to Z_{eu}. The resultant P_z profile falls between the profiles calculated for the two vertically uniform light-limited slopes (Fig. 3). In situ, the existence of a deep chlorophyll maximum will tend to increase the sensitivity of $\Sigma\ PP$ to depth-dependent photoadaptation over that calculated here. However, vertical variability in the light-limited slope is typically less than the factor of six used in our calculations, such that variability in E_k^* has a smaller effect on Σ
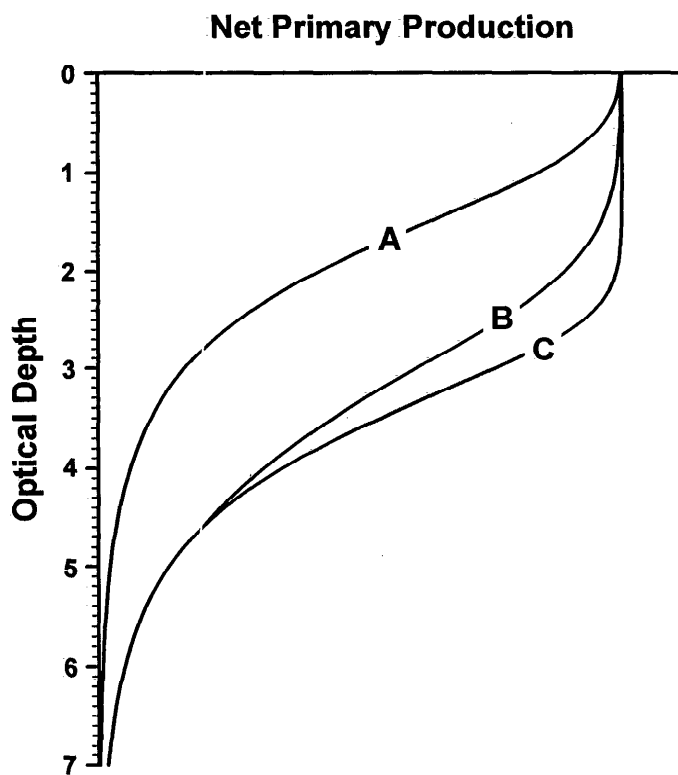

Net Primary Production

Fig. 3. Effect of varying the saturation irradiance (E_k^*) on modeled vertical profiles of net primary production (P_z). Identical maximum values (P^b_{opt}) are assumed for each P_z profile, and thus changes in E_k^* result from variability in the light-limited slope for photosynthesis. Vertically uniform values for E_k^* were used to calculate profiles A and C, with E_k^* for profile C being a factor of 6 greater than for profile A (i.e. the maximum range expected in situ). Profile B results when E_k^* is assumed to increase six-fold from the surface to the depth of the euphotic zone (4.6 o.d.). The shape of each P_z profile is a function of daily surface irradiance (E_0). Thus, differences in depth-integrated net primary production ($\Sigma\ PP$) between profiles are E_0 dependent, with $\Sigma\ PP$ for profiles A and C differing by a factor of ~1.5–3 for E_0 ranging from 65 to 5 mol quanta m^{-2}, respectively.

PP in situ. Thus, we can conclude that variability in E_k^* typically causes $\Sigma\ PP$ to vary by a maximum of a factor of <3, which represents only a fraction of the ~10% variance in $\Sigma\ PP$ not accounted for by Eq. 12 and C_z. Consequently, the potential for improving $\Sigma\ PP$ estimates using a vertically resolved model over a DIM is negligible.

Ranking the importance of productivity model variables

Variability in $\Sigma\ PP$ spans more than three orders of magnitude globally (~30–10,000 mg C m^{-2} d^{-1}) and results primarily from changes in depth-integrated phytoplankton biomass ($\Sigma\ C$), which ranges from ~2 to 500 mg Chl m^{-2}. Reasonable values for P^b_{opt} vary within a factor of ~40 (Behrenfeld and Falkowski 1997), ranging from ~0.5 to 20 mg C (mg Chl)$^{-1}$ h^{-1}. Typically, α^b and P^b_{max} vary by factors of ~6 and ~25 (Falkowski 1981), respectively. Thus, the potential variability in E_k is on the order of a factor of ~240.

However, Platt and Sathyendranath (1993) observed that E_k varied by only a factor of ~ 12 and I_*^m by only a factor of 6–8, due to strong positive correlations between α^b and P^b_{max} and E_0 and E_k (*see* also Eq. 31). Because I_*^m is proportional to E_0/E_k^* and $\Sigma\ PP$ varies as a function of E_k^* according to $\ln(E_0/E_k^*)$, the observed range for I_*^m indicates that spatial variability in E_k^* contributes roughly a factor of ~ 1.5–2 to variability in $\Sigma\ PP$. Neglecting very low values of E_0/E_k^*, Fig. 2 indicates that E_0-dependent changes in the depth of light saturation can potentially cause $\Sigma\ PP$ to vary by a factor of ~ 4, but more commonly by a factor of <2 (*see* shaded area in Fig. 2). Daylength has only a minor effect on variability in $\Sigma\ PP$. Thus, we can rank the importance of standard productivity model variables as

$$\Sigma\ C \gg P^b_{opt} \gg E_k^* \approx E_0 > DL.$$

Similar conclusions were drawn from previous analyses of variability within two large observational datasets (Balch and Byrne 1994; Behrenfeld and Falkowski 1997).

Models of P^b_{opt}

We have discussed above the contribution of E_k^* and E_0 to variability in $\Sigma\ PP$, but have neglected the far more significant influence of variability in P^b_{opt}. In this section, we present an overview of the diverse parameterizations used for P^b_{opt}. Despite this diversity, P^b_{opt} remains the most poorly described variable in any $\Sigma\ PP$ model, such that current parameterizations are performing relatively well if they account for 20% of the variability observed.

As an initial estimate, Ryther and Yentsch (1957) assigned P^b_{opt} a constant value of 3.7 mg C (mg Chl)$^{-1}$ h^{-1}, which Cullen (1990) suggested should be revised to 4.8 mg C (mg Chl)$^{-1}$ h^{-1} due to improvements in the determination of pigment concentrations. Likewise, a constant value for P^b_{opt} of ~ 2.5 mg C (mg Chl)$^{-1}$ h^{-1} is implicit in the ψ model of Falkowski (1981) (Fig. 4).

Megard (1972) presented the first variable model for P^b_{opt}, describing it as a function of surface water temperature (T°) in °C:

$$P^b_{opt} = 0.118 \times T^\circ + 1.25. \tag{32}$$

In Eq. 32, we have divided Megard's original equation by the average daylength for his study (13.7 h) to express P^b_{opt} as an hourly rate (Fig. 4). In the same year, Eppley (1972) compiled results from numerous laboratory studies to describe a temperature-dependent function for the maximum achievable specific growth rate of phytoplankton (μ_{max}),

$$\mu_{max} = 10^{0.0275 \times T^\circ - 0.07}, \tag{33}$$

which subsequently has been implemented in numerous Σ PP models by assuming a constant carbon-to-chlorophyll ratio (Fig. 4). Applying Eq. 33 to calculations of $\Sigma\ PP$ implies that resultant estimates represent maximum achievable values, not the average values they are often treated as. In contrast, Behrenfeld and Falkowski (1997) described a temperature-dependent function for the median value of P^b_{opt} (Fig. 4). Their equation was based on fitting a polynomial to observational data and improved the explained variance in P^b_{opt}

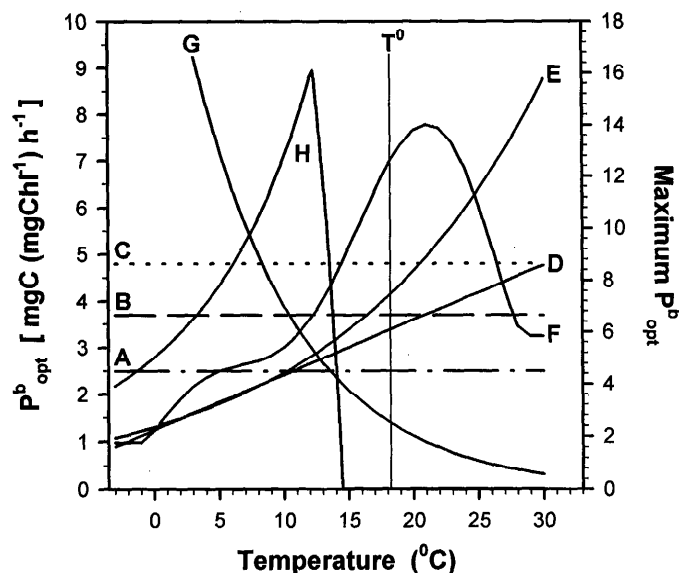
Fig. 4. Summary of published models for estimating the maximum chlorophyll-specific carbon fixation rate within a water column (P^b_{opt}). A = calculated value implicit in the ψ model of Falkowski (1981). B = Ryther and Yentsch's (1957) estimate of 3.7 mg C (mg Chl)$^{-1}$ h^{-1}. C = Cullen's (1990) revised value for B of 4.8 mg C (mg Chl)$^{-1}$ h^{-1}. D = Megard's (1972) model converted to hourly rates by dividing by 13.7 h (Eq. 32). E = Eppley's (1972) equation for the maximum specific growth rates (Eq. 33) converted to carbon fixation by normalizing to 4.6 mg C (mg Chl)$^{-1}$ h^{-1} at 20°C following Antoine et al. (1996). F = Behrenfeld and Falkowski's (1997) seventh-order polynomial model. G = Balch et al. (1992) (Eq. 34). H = Biphasic model of Balch and Byrne (1994) for the maximum achievable P^b_{opt} calculated for 20–30° latitude using a carbon:chlorophyll ratio of 150 and expressed in units of mg C (mg Chl)$^{-1}$ h^{-1} (*see* their Fig. 6). The left axis applies to models A–G and the right axis to model H. T° = Levitus climatological median upper ocean temperature (18.1°C) as computed by Antoine et al. (1996).

by $\sim 60\%$ over Eq. 33 for their dataset, which in absolute terms amounted to a correlation coefficient of only 0.24.

In 1992, Balch et al. described the product of P^b_{opt} and DL as

$$P^b_{opt} \times DL = 10^{-0.054 \times T^\circ + 2.21}. \tag{34}$$

Equation 34 illustrates quite clearly that not only is a consensus lacking on the general shape of the proper P^b_{opt} function, but there is not even agreement on the appropriate sign of the slope! Finally, Balch and Byrne (1994) described P^b_{opt} as a biphasic function of both temperature and nutrient concentration (Fig. 4). They used Eppley's temperature-dependent function (Eq. 33) to describe P^b_{opt} at low temperatures and a Michaelis–Menten relationship to reduce P^b_{opt} at higher temperatures where nitrate concentrations were expected to become limiting. Like Eq. 33, this biphasic function described a maximum envelope rather than a mean.

An alternative approach to modeling P^b_{opt} has been the description of geographically defined oceanic provinces with seasonally uniform photoadaptive states characterized from historical databases of photosynthesis–irradiance measurements. In the most recent compilation, Longhurst et al. (1995) characterized seasonal variability in photoadaptive

variables for 57 biogeographical provinces. Like all P^b_{opt} models, provincial characterizations explain a limited amount of variability in P^b_{opt}, such that variability within a given province commonly exceeds differences between provinces (Platt et al. 1991).

Estimates of global phytoplankton productivity

A common application of productivity models is the calculation of global annual phytoplankton primary production (PP_{annu}). Published estimates of PP_{annu} vary from 27.1 (Eppley and Peterson 1979) to 50.2 Pg C yr^{-1} (Longhurst et al. 1995). Although calculations of PP_{annu} from daily Σ PP models should amplify any systematic differences between models, this discrepancy between published PP_{annu} estimates would at first appear too large to support our earlier conclusion that fundamental differences between models have only a minor effect on Σ PP calculations. However, further investigation reveals that these discrepancies are due primarily to differences in input chlorophyll fields. Eppley and Peterson (1979) estimated PP_{annu} using chlorophyll distributions derived by Platt and Subba Rao (1975) from shipboard observations that underestimated global phytoplankton biomass compared to satellite data. In contrast, the highest value of 50.2 pg C yr^{-1} was based on satellite chlorophyll fields derived using a biomass retrieval algorithm (Sathyendranath and Platt 1989*b*) that produces higher chlorophyll concentrations than the NASA standard algorithm used by most researchers. When compared over the North Atlantic basin (Platt et al. 1991), this alternative algorithm resulted in CZCS-based surface chlorophyll concentrations that were on average ~100% higher than values produced by NASA standard algorithm. Behrenfeld and Falkowski (1997) used the standard NASA chlorophyll data and Eq. 12 to estimate PP_{annu} at 43.5 Pg C yr^{-1}. These same chlorophyll fields were used in a WRM by Antoine et al. (1996) to estimate PP_{annu} at 46.9 Pg C yr^{-1}. Thus, the minor differences expected between Σ PP models were realized once input chlorophyll data were standardized.

Synthesis

We partitioned variability in Σ PP into that associated with each variable in the standard DIM (Eq. 11) and found that nearly all (~85%) could be attributed to changes in depth-integrated biomass (i.e. $C_{sat} \times Z_{eu}$) and spatial (i.e. horizontal) variability in the photoadaptive variable P^b_{opt}. Only a small fraction (<15%) of variability in Σ PP can be attributed to the cumulative effect of E_0-dependent changes in the depth of light saturation (F), spatial variability in E_k^*, and vertical variability in C_z and E_k^*. Because it is the variable description of the vertically resolved factors that distinguishes different categories of Σ PP models, it appears that the potential for improvements in Σ PP estimates between categories is negligible, so long as equivalent parameterizations are used between models for the horizontal variability in P^b_{opt} and E_k^* and a linear dependence on E_0 is not assumed.

That variability in E_0 explains a relatively minor portion of the variability in Σ PP is perhaps the most counterintu-

itive result of our investigation, because the effect of E_0 on P_z is so clear that any biological oceanographer or limnologist could differentiate between P_z profiles from low-light and high-light conditions without any additional information. However, this unavoidable conclusion is a consequence of the exponential attenuation of E_z restricting the effect of the full range in E_0 on variability in Σ PP to a small fraction of that attributable to variability in P^b_{opt} and Σ C. Specifically, changes in E_0 typically contribute a factor of ~2 to variability in Σ PP, which is a small fraction of the three orders of magnitude variability observed in Σ PP.

The widespread use of light as the principal forcing component in Σ PP models is understandable, because physical processes governing the wavelength-specific distribution of light in the world's oceans are well characterized and easily rendered into mathematical formulations and computer code. Consequently, models have been developed with the capacity to relate production at any depth to the spectrally dependent absorption of time-dependent irradiance. Conceivably, this reductionist approach could be continued ad infinitum but with negligible benefits toward improving model estimates of Σ PP.

The intent of this report was not to diminish the important advances made in the development of WRMs, for such models provide a sound foundation for developing mechanistic productivity models once a better understanding of algal physiology has been achieved. Rather, we hope this analysis demonstrates the fundamental synonymy between models and will help usher the productivity modeling community into abandoning a long history of parallel and redundant modeling efforts By doing so, a more focused effort can be made in the future on understanding the underlying causes of variability in physiological factors most influential on variability in depth-integrated phytoplankton productivity.

References

ANTOINE, D., J.-M. ANDRÉ, AND A. MOREL. 1996. Oceanic primary production 2. Estimation at global scale from satellite (coastal zone color scanner) chlorophyll. Global Biogeochem. Cycles **10:** 57–69.

BALCH, W. M., AND C. F. BYRNE. 1994. Factors affecting the estimate of primary production from space. J. Geophys. Res. **99(C4):** 7555–7570.

―――, R. EVANS, J. BROWN, G. FELDMAN, C. MCCLAIN, AND W. ESAIAS. 1992. The remote sensing of ocean primary productivity: Use of new data compilation to test satellite models. J. Geophys. Res. **97(C2):** 2279–2293.

BANNISTER, T. T. 1974. Production equations in terms of chlorophyll concentration, quantum yield, and upper limit to production. Limnol. Oceanogr. **19:** 1–12.

BANSE, K., AND M. YONG. 1990. Sources of variability in satellite-derived estimates of phytoplankton production in the Eastern Tropical Pacific. J. Geophys. Res. **95(C5):** 7201–7215.

BEHRENFELD, M. J., AND P. G. FALKOWSKI. 1997. Photosynthetic rates derived from satellite-based chlorophyll concentrations. Limnol. Oceanogr. **42:** 1–20.

BIDIGARE, R. R., B. B. PRÉZELIN, AND R. C. SMITH. 1992. Bio-optical models and the problems of scaling, p. 175–212. *In* P. G. Falkowski and A. D. Woodhead [eds.], Primary productivity and biogeochemical cycles in the sea. Plenum.

CULLEN, J. J. 1990. On models of growth and photosynthesis in phytoplankton. Deep-Sea Res. **37:** 667–683.

DRING, M. J., AND D. H. JEWSON. 1982. What does ^{14}C uptake by phytoplankton really measure? A theoretical modelling approach. Proc. R. Soc. Lond. **214:** 351–368.

DUBINSKY, Z. 1992. The functional and optical absorption cross sections of phytoplankton photosynthesis, p. 31–45. *In* P. G. Falkowski and A. D. Woodhead [eds.], Primary productivity and biogeochemical cycles in the sea. Environ. Sci. Res. V. 43. Plenum.

EPPLEY, R. W. 1972. Temperature and phytoplankton growth in the sea. Fish. Bull. **70:** 1063–1085.

————, AND B. J. PETERSON. 1979. Particulate organic matter flux and planktonic new production in the deep ocean. Nature **282:** 677–680.

————, E. STEWART, R. M. ABBOT, AND V. HEYMAN. 1985. Estimating ocean primary production from satellite chlorophyll, introduction to regional differences and statistics for the Southern California Bight. J. Plankton Res. **7:** 57–70.

FALKOWSKI, P. G. 1981. Light-shade adaptation and assimilation numbers. J. Plankton Res. **3:** 203–216.

————. 1992. Molecular ecology of phytoplankton photosynthesis, p. 47–67. *In* P. G. Falkowski and A. D. Woodhead [eds.], Primary productivity and biogeochemical cycles in the sea. Environ. Sci. Res. V. 43. Plenum.

GEIDER, R. J., AND B. A. OSBORNE. 1992. Algal photosynthesis. Chapman and Hall.

JASSBY, A. D., AND T. PLATT. 1976. Mathematical formulation of the relationship between photosynthesis and light for phytoplankton. Limnol. Oceanogr. **21:** 540–547.

LINDEMAN, R. L. 1942. The trophic-dynamic aspect of ecology. Ecology **23:** 399–418.

LONGHURST, A., S. SATHYENDRANATH, T. PLATT, AND C. CAVERHILL. 1995. An estimate of global primary production in the ocean from satellite radiometer data. J. Plankton Res. **17:** 1245–1271.

LORENZEN, C. J. 1972. Extinction of light in the ocean by phytoplankton. J. Cons. Cons. Int. Explor. Mer. **34:** 262–267.

LORENZEN, M. 1972. The role of artificial mixing in eutrophication control. Ph.D. thesis, Harvard Univ.

MEGARD, R. O. 1972. Phytoplankton, photosynthesis, and phosphorus in Lake Minnetonka, Minnesota. Limnol. Oceanogr. **17:** 68–87.

MOREL, A. 1978. Available, usable, and stored radiant energy in relation to marine photosynthesis. Deep-Sea Res. **25:** 673–688.

————. 1991. Light and marine photosynthesis: A spectral model with geochemical and climatological implications. Prog. Oceanogr. **26:** 263–306.

————, AND J.-F. BERTHON. 1989. Surface pigments, algal biomass profiles, and potential production of the euphotic layer: Relationships reinvestigated in view of remote-sensing applications. Limnol. Oceanogr. **34:** 1545–1562.

PLATT, T. 1986. Primary production of the ocean water column as a function of surface light intensity: Models for remote sensing. Deep-Sea Res. **33:** 149–163.

————, C. CAVERHILL, AND S. SATHYENDRANATH. 1991. Basin-scale estimates of oceanic primary production by remote sensing: The North Atlantic. J. Geophys. Res. **96:** 15147–15159.

————, AND B. IRWIN. 1973. Caloric content of phytoplankton. Limnol. Oceanogr. **18:** 306–310.

————, AND S. SATHYENDRANATH. 1988. Oceanic primary production: Estimation by remote sensing at local and regional scales. Science **241:** 1613–1620.

————, AND ————. 1993. Estimators of primary production for interpretation of remotely sensed data on ocean color. J. Geophys. Res. **98:** 14,561–14,567.

————, AND D. V. SUBBA RAO. 1975. Primary production of marine microphytes, p. 249–280. *In* J. P. Cooper [ed.], Photosynthesis and productivity in different environments. Cambridge Univ.

RODHE, W. 1966. Standard correlations between pelagic photosynthesis and light, p. 367–381. *In* C. R. Goldman [ed.], Primary productivity in aquatic environments. Univ. Calif.

————, R. A. VOLLENWEIDER, AND A. NAUWERK. 1958. The primary production and standing crop of phytoplankton, p. 299–322. *In* A. A. Buzzati-Traverso [ed.], Perspectives in marine biology. Univ. Calif.

RYTHER, J. H. 1956. Photosynthesis in the ocean as a function of light intensity. Limnol. Oceanogr. **1:** 61–70.

————, AND C. S. YENTSCH. 1957. The estimation of phytoplankton production in the ocean from chlorophyll and light data. Limnol. Oceanogr. **2:** 281–286.

SAKSHAUG, E., K. ANDRESEN, AND D. A. KIEFER. 1989. A steady state description of growth and light absorption in the marine planktonic diatom *Skeletonema costatum*. Limnol. Oceanogr. **34:** 198–205.

SATHYENDRANATH, S., AND T. PLATT. 1989*a*. Computation of aquatic primary production: Extended formalism to include effect of angular and spectral distribution of light. Limnol. Oceanogr. **34:** 188–198.

————, AND ————. 1989*b*. Remote sensing of ocean chlorophyll: Consequence of non-uniform pigment profile. Appl. Opt. **28:** 490–495.

————, ————, C. M. CAVERHILL, R. E. WARNOCK, AND M. R. LEWIS. 1989. Remote sensing of oceanic primary production: Computations using a spectral model. Deep-Sea Res. **36:** 431–453.

SMITH, E. L. 1936. Photosynthesis in relation to light and carbon dioxide. Proc. Natl. Acad. Sci., USA **22:** 504–511.

SMITH, R. C., AND K. S. BAKER. 1978. The bio-optical state of ocean waters and remote sensing. Limnol. Oceanogr. **23:** 247–259.

TALLING, J. F. 1957. The phytoplankton population as a compound photosynthetic system. New Phytol. **56:** 133–149.

————. 1970. Generalized and specialized features of phytoplankton as a form of photosynthetic cover, p. 431–435. *In* Prediction and measurement of photosynthetic productivity. Proc. IBP/PP Tech. Meeting Třeboň (Czechoslovakia). Centre Agr. Publ. Doc., Wageningen.

VOLLENWEIDER, R. A. 1966. Calculation models of photosynthesis–depth curves and some implications regarding day rate estimates in primary production measurements, p. 426–457. *In* C. R. Goldman [ed.], Primary productivity in aquatic environments. Univ. Calif.

————. 1970. Models for calculating integral photosynthesis and some implications regarding structural properties of the community metabolism of aquatic systems, p. 455–472. *In* Prediction and measurement of photosynthetic productivity. Proc. IBP/PP Tech. Meeting Třeboň (Czechoslovakia). Centre Agr. Publ. Doc., Wageningen.

WRIGHT, J. C. 1959. Limnology of Canyon Ferry Reservoir: Phytoplankton standing crop and primary production. Limnol. Oceanogr. **4:** 235–245.